Asian Journal of Chemistry; Vol. 33, No. 5 (2021), 1039-1050

ASIAN JOURNAL OF CHEMISTRY

https://doi.org/10.14233/ajchem.2021.23157

Overview of Electrode Materials Progressed for Application in Electrochemical Supercapacitors: An Update

VINAYA JOSE, VISMAYA JOSE and A. SAMSON NESARAJ*

Department of Applied Chemistry, Karunya Institute of Technology and Sciences (Deemed to be University), Karunya Nagar, Coimbatore-641114, India

*Corresponding author: E-mail: drsamson@karunya.edu

Received: 8 February 2021; *Accepted*: 23 February 2021; *Published online*: 16 April 2021; AJC-20323

Supercapacitors are the most maintainable energy conservation devices and have pulled in broad consideration due to long cycle life, excellent power density, stability and integrity. As of now, all researchers are concentrating on how the energy density can be improved while retaining high power density, fast charge or discharge and cycling stability. In this review, we look into the most broadly used electrode materials based on carbon nanotubes (CNTs), graphene, activated carbon, carbon quantum dots, porous carbon, metal oxides, conducting polymers, composite hybrid materials, asymmetric hybrid materials, battery type electrode materials, *etc.* for designing various types of supercapacitors and their characteristic performance. This review would help to understand the recent advancements progressed in electrode materials for applications in electrochemical supercapacitors.

Keywords: Carbon, Metal oxide, Polymer, Hybrid, Electrode materials, Supercapacitors.

INTRODUCTION

Since the discovery of electricity, we have looked for compelling strategies to store that energy to utilize on request. It is critical to create environmentally sustainable energy-production and storage technologies [1]. Supercapacitors are the most maintainable energy conservation devices and have pulled in broad consideration due to long cycle life [2], excellent power density, stability and integrity [3]. Capacitors can discharge the energy at a much greater rate than batteries, there's no chemical reaction required to charge or release a supercapacitor, so it can be charged and discharged exceptionally rapidly [4-6]. Supercapacitors are divided into three, depending on the energy storage mechanism (Fig. 1). To begin with one is electrical double layer capacitor (EDLC), which is able to charge or discharge the energy inside a brief time with good energy storage performances. Second group is pseudocapacitors, which stores energy through reversible faradaic charge transfer, which includes quick and reversible redox reactions on the electrode-electrolyte interface [7,8]. The final category is hybrid, which blends both EDLC and pseudocapacitor properties [9].

Low energy density, cost of production, low voltage per cell and high self-discharge are among the difficulties confronted by supercapacitors [10]. Among the best techniques to controlling the deterrent of low energy density is by creating new electrode materials for designing supercapacitors. Choice of electrode material is fundamental significance in the construction of supercapacitors because it decides the electrical properties [11]. Carbon materials, metal oxides and conducting polymers are the well-known electrode materials for supercapacitors [12]. Due to their large surface area, carbon materials have been used since the beginning of supercapacitor development [13]. Metal oxides have received broad consideration due to large specific capacitance and low resistance, help to develop supercapacitors of excellent energy storage performances [14,15]. Electrochemical redox reaction is utilized to store the energy in case of conducting polymers. There are numerous applications utilize supercapacitors as storage devices for energy. It can be utilized in sound hardware, continuous control supplies, lasers, camera beams, beat loads such as magnetic coils, *etc*. In fields such as computer memory reinforcement, electric vehicles, regenerative braking in the mechanical

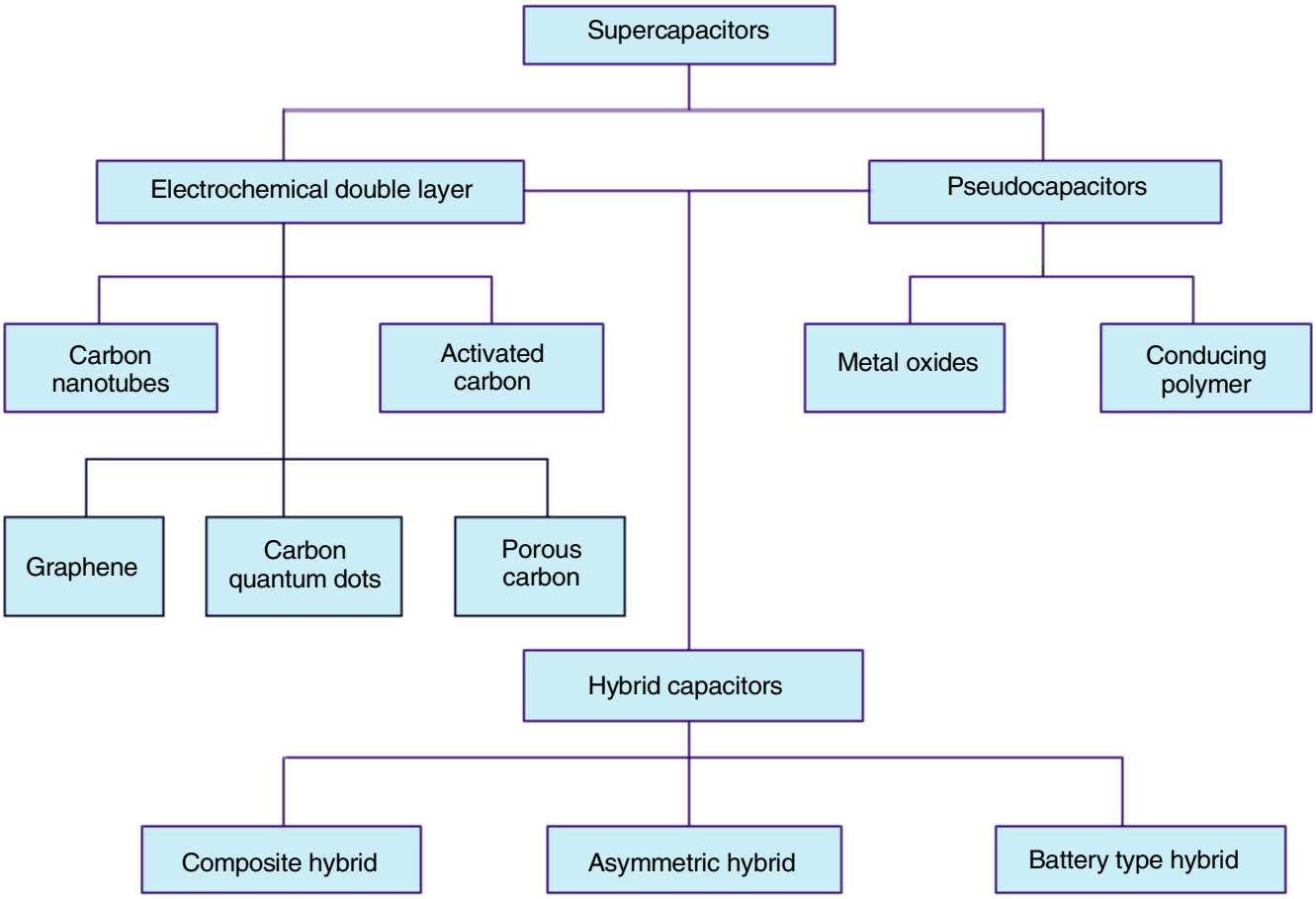

Fig. 1. Classification of supercapacitors

electric motors and automobile industry, during power loss and numerous others, it can store vast quantities of energy and deliver modern technical prospects [2,16,17].

As of now, all researchers are concentrating on the improvement of the energy density while retaining high power density, fast charge or discharge and cycling stability. In this review, the most broadly used electrode materials for designing various types of supercapacitors and their characteristic performance are discussed. This review would help to understand the recent advancements progressed in electrode materials for application in electrochemical supercapacitors.

Design and working principle of a supercapacitor: Supercapacitor has two plates which are isolated by an ion-permeable layer (separator) and an electrolyte ionically interfacing both electrodes [18]. The plates are made of metal coated with a porous material such as powdery, activated charcoal, which allows them a greater area for more charge storage effectively [19,20]. As the electrodes are polarized by an applied voltage, electrolyte ions form electrical double layers with the opposite polarity to the electrode polarity, making electric field between them [21]. For instance, at the electrode/electrolyte interface, positively polarized electrodes would have a layer of negative ions along with a charge-balancing layer of positive ions that adsorb onto the negative layer. For negative electrodes, the reverse holds true. The field polarizes the dielectric, so that its molecules line up in the opposite direction to the field, decreasing its property [22].

Supercapacitors store energy in the form of electrostatic charges between two conductive terminals, isolated by a dielectric material [23]. The eletrodes in supercapacitors are permeable. The energy stored in an supercapacitor (E_{SC}) is given by the following equation:

$$E_{SC} = ½ CV^2 \quad (1)$$

where C = capacitance and V = voltage between terminals.

The capacitance in turn is proportional to the electrode area. So, utilizing porous electrodes gives a large specific area with a consequent high energy density [24]. Energy storage mechanism of electrochemical double-layer capacitor is shown in Fig. 2.

Electrode materials

Electrochemical double-layer capacitors (EDLCs): Electrochemical double-layer capacitors are constructed as electrodes using two carbon-based materials, an electrolyte and a separator [25]. Like traditional capacitors, EDLCs too store energy through charge separation, which leads to double-layer capacitance [26]. It comprises two distinct layers of charge separately at the interface between electrolytes with positive electrodes and negative electrodes. The division between electrical double layers in an EDLC is lower than that in a traditional capacitor [27,28]. It can store charge electrostatically or through a non-faradaic process, which does not include the charge exchange between the electrode and the electrolyte [29].

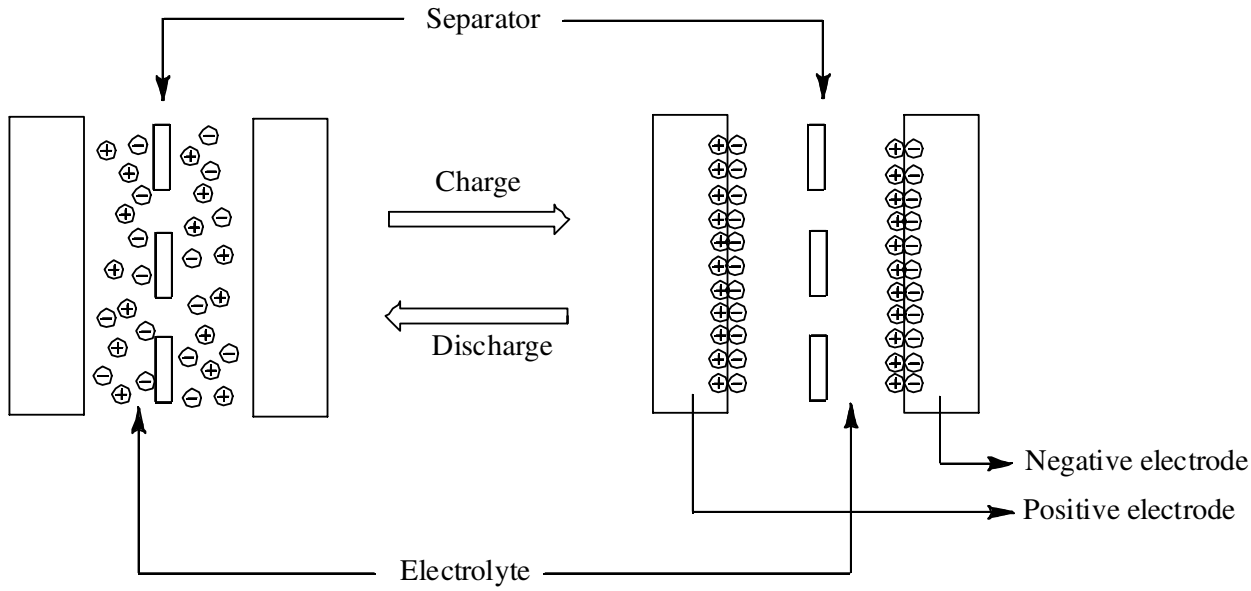

Fig. 2. Storage mechanism of electrochemical double-layer capacitor [Ref. 25]

When voltage is connected, there is an aggregation of charge on electrode surfaces due to the difference in potential, which leads to attraction of opposite charges. These occur in electrolyte ions that scatter over the separator and pores of the opposite charged electrode [30]. In order to prevent the recombination of ions on the electrode, it is necessary to form a double-layer charge [31]. The double layer, combined with the increment in particular surface area and separations between electrodes diminished, permits EDLCs to accomplish grater energy density [32]. It is able to charge or discharge inside a brief time with good energy performance [33]. In this scenario, EDLCs demand electrode materials with a large specific surface area and great electrical conductivity, which can be satisfied particularly by carbon nanotubes (CNTs), graphene, activated carbon, carbon quantum dots (CQDs) and porous carbon (Fig. 1) [34].

Carbon nanotubes (CNTs): Carbon nanotube is a one-dimensional nanostructures of tubular-shaped carbon materials [35], which shows excellent physical and chemical properties such as mechanical strength, electrical conductivity and specific surface area. It can be used within the development of composites based on CNT to increase the capacity of energy storage [3]. Carbon nanotube is delivered by the catalytic splitting up of several hydrocarbons and through careful control of different parameters. It is conceivable to create nanostructures in different structures and additionally direct their crystal structures. Carbon nanotube has interconnected mesopores, unlike other carbon electrode materials, which permits for the continuous charge dispersion that uses entire available surface areas [36]. It is mainly classified as single-walled carbon nanotubes (SWCNTs) and multi-walled carbon nanotubes (MWCNTs) [3,4,22]. Single-walled carbon nanotubes have been achieved a specific capacitance of 180 F g^{-1}, power density of 20 kW Kg^{-1} and energy density of 7 Wh kg^{-1}. CNT diameter plays an important role in regulating the intrinsic surface area. The multiwalled carbon nanotubes (MWNTs) changed their specific surface area from 128 to 411 m^2 g^{-1} with external diameter of 10 to 20 nm and internal diameter of 2 to 5 nm. The highest specific capacitance of MWCNTs is found to be 80 F g^{-1} in 6 M KOH electrolyte [37].

Graphene: Graphene has two-dimensional crystalline carbon shape and their single coating of carbon atoms form a grid of honeycomb or many coupling layers of the framework of honeycomb [38]. The term graphene typically indicates single-layer graphene when utilized without indicating the shape as bilayer graphene, multilayer graphene [39]. There are two sub-lattices in the honeycomb cross section of graphene, so that every particles in one sub-lattice is encompassed of three particles in other sub-lattice and *vice versa* [40]. This basic structure gives the impression that the electrons and gaps in graphene show abnormal degree of internal freedom, more often than not called pseudo-spin [41,42]. Graphene is considered exceptionally promising for numerous such applications. It is being electrically conducting, clear, solid and adaptable, which can be an imminent medium in touchpads [43]. Moreover, it shows excellent thermal conductivity and can be used to separate heat from electronic systems [44]. Being mechanically very solid, which may be utilized as a framework to examine biomolecules and numerous substrates. It has been recently suggested that the graphene can be utilized in energy storage devices, since it doesn't rely on the arrangement of pores at the solid state, when compared to other carbon materials including porous carbon, activated carbon, carbon quantum dots, carbon nanotube, *etc.* [45]. Most carbon materials can be used as electrode materials, the recently created graphene has a relatively high specific surface area (SSA) of about 2630 m^2 g^{-1}. In case the complete SSA is completely used graphene has the potential to accomplish a capacitance of up to 550 F g^{-1} [46]. These extraordinary properties have inspired various efforts to use graphene as electrode material in supercapacitors. Three separate methods were studied to discover a more effective method for utilizing graphene as electrode materials. The first technique was graphic oxide thermal exfoliation, graphene was retrieved in the second strategy by heating nano-diamond

in a helium atmosphere at 1650 ºC and decomposition over nickel nanoparticles was within the final method of camphor. Thermal exfoliation of graphitic oxide has recorded specific capacitance and energy density are 117F g^{-1} and 31.9 Wh kg^{-1}, respectively [47].

Cheng *et al*. [48] synthesized MnO_2 nanowire/graphene composite (MGC) as positive electrode and graphene as negative electrode in a neutral aqueous Na_2SO_4 solution as electrolyte. Solution-phase assembly of graphene layers and α-MnO_2 nanotubes was used to arrange the MGC. Those asymmetric electrical double-layer capacitors can be reversed within the high-voltage range of 0-2.0 V and display good energy density of 30.4 Wh kg^{-1}. The graphene-electrode materials can be used in electrolyte-based asymmetric capacitors with good energy storage performances [48]. Graphene nanoplate-MnO_2 composites have been synthesized by Huang *et al.* [49] by oxidizing portion of the carbon molecules within the scaffold of graphene nanowires at normal temperature. The graphene sheets of the samples obtained at 1 and 3 h were relatively smooth and decorated by only a small quantity of MnO_2 nanoparticles. As an electrode material, the nanocomposite arranged within the reaction time of 3 h uncovers way better energy storage performances compared to MnO_2 nanolamellas [49]. Dai *et al.* [50] synthesized graphene oxide (GO) nanosheet/MnO_2 nanowire hybrid has excellent consistency through the hydrothermal method. The great electrochemical performance of as-prepared GO/MnO_2 hybrids was obtained due to the unique chemical interactions between GO and MnO_2. Graphene oxide (GO) nanosheets/MnO_2 primarily utilized for potential applications in energy storage and conversion gadgets.

Activated carbon: Activated carbon can be broadly utilized as electrode materials in electrochemical capacitors since of their simple synthesis, production cost and good electrical conductivity [51]. It has been created from different kind of carbon based materials such as wood, coal nutshell, *etc*. by either physical or chemical actuaution [52]. Activated carbon is more often than not induced from charcoal and utilized in air purification, gold purification, metal extraction, solvent recovery, water purification, medication, methane and hydrogen storage, drain treatment, filters in compressed and respirators, teeth brightening, hydrogen chloride generation and numerous other applications [53]. The high temperature (700-1200 ºC) method of carbon precursors within the presence of oxidizing gases such as moisture, CO_2 and air, which leads to physical stimulation [54]. The activated carbon is saturated with particular chemicals [55]. This chemical is generally an acid, base or salt such as KOH (5%), NaOH (5%), phosphoric acid (25%), $ZnCl_2$ (25%) and $CaCl_2$ (25%). At that point, it is forced to lower temperature range of 250-600 ºC. It is generally accepted that temperature stimulates carbon in this range by driving the material to open and have greater micropores [56]. Here, electrochemical capacitor utilizes carbon based composite, invloving an exceptionally high surface area, high purity activated carbon to keep electrolyte inside its permeability [57]. The electrolyte can quickly be charged with electrons as they went through energy is recovered and keep it with negligible discharge and a power distant in excess of its own mass. The activated carbon permits the discharge of stored energy quickly without loss of energy, in turn retrieving required capacity to electrochemical cell. This indicates the supercapacitor can be charged and discharged over and over for large number of cycles without loss of optimal capacity [58].

Carbon quantum dots (CQDs): Carbon quantum dots are a new type of fluorescent tiny carbon nanoparticles with a particle size of less than 10 nm, which has broad application prospects [34]. Carbon quantum dots have potential applications in the field of fluorescence, bioimaging, drug delivery, synthetic chemistry, material science and energy capacity. These materials are low- hazardous, water soluble, so cheap, physico-chemically and photochemically stable and have great biocompatibility [59]. Kakaei *et al.* [60] synthesized CQDs/PANI composite as great electrode material for high performance supercapacitors. The composite materials are arranged by adsorbing C-dots on polyaniline (PANI). The obtained composite material appears great performance for supercapacitors with a high specific capacitance of 264.6 F g^{-1} at a current density of 2.5 A g^{-1}.

Newly carbon quantum dots (CQDs) have zero-dimensional nanostructures, which have received broad consideration in electrochemical energy capacity. An electrochemical synthetic route was used to develop flexible all-solid-state supercapacitors (ASSSs) by one step co-deposition of suitable quantities of pyrrole monomer and CQDs in aqueous solution. The prepared CQD/PPy composite ASSS has excellent capacitance performance, great specific capacitance of 315 mF cm^{-2} at a current density of 0.2 mA cm^{-2} and a long-life cycle stability of 2000 continuous cycles. This result showed that electrochemically synthesized CQDs/PPy composite material as the electrode material of supercapacitors may be a new method to improve flexible electronic devices [61]. Carbon quantum dots (CQDs) tuned porous $NiCo_2O_4$ spheres composites are developed by Zhu *et al*. [62] by means of a reflux synthesis method taken after by a post annealing treatment. The CQDs/$NiCo_2O_4$ composite electrode shows excellent specific capacitance (856 Fg^{-1} at 1 Ag^{-1}). The assembled AC//CQDs/$NiCo_2O_4$ asymmetric supercapacitor shows high energy density and power density are 27.8 Wh kg^{-1} and 10.24 kW kg^{-1}, respectively and also remarkable cycling stability of101.9% of the initial capacity retention over 5000 cycles at 3 Ag^{-1}. These interesting results indicate that CQDs/$NiCo_2O_4$ composites are expected to be excellent candidate electrode materials for high-performance energy capacity gadgets [62]. Lv *et al*. [63] synthesized the CQD aerogel with a specific surface area (1027 m^2 g^{-1}) by assembling CQD *in situ* by sol-gel polymerization of resorcinol (R) and formaldehyde (F). Since the surface has carboxyl and hydroxyl groups, CQD can be easily connected to the RF polymer system. The anchored CQDs developed the CQD-free carbon aerogel's electrochemical capacitive property and the CQD aerogel electrodes appeared high specific capacitance of 294.7 F g^{-1} at a current density of 0.5 A g^{-1}. So the result clearly proved that CQD aerogel is an ideal fabric for high-performance supercapacitor applications.

A facile hydrothermal route is accepted for the preparation of hierarchical flower like NiS nanostructure materials with carbon quantum dot (NiS/C-dot) composite [64]. The composite

fabric has shown excellent performance as a supercapacitor in electrochemical energy storage systems, with a specific capacity 880 F g^{-1}. The material remained stable during the 2000 charge-discharge cycles tested. From normal sources, carbon quantum dots with size 1.3 nm were formed and C-dots were used for the supercapacitor performance of NiS.

Zhou and Xie [65] developed carbon-doped quantum dots and iron-coordinated polypyrrole (CQDs/PPy-Fe) as an excellent electrode material for supercapacitors. The CQDs/PPy-Fe was arranged by introducing CQDs into PPy-Fe that was synthesized by electropolymerization of pyrrole monomer coordinated by ferrous chloride. At 20.0 A g^{-1}, the capacitance retention rates of CQDs/PPy-Fe and PPy after 2000 cycles were 94.6% and 79.4%, respectively. The plan of CQDs/PPy-Fe presents the excellent candidate for electrochemical energy storage devices. Manganese oxides/graphene composite material has come to be provided as a good electrode material for supercapacitors. Here, carbon quantum dots provide a bridge for connecting MnO_2 and graphene, which helps to develop stable MnO_2/carbon quantum dot/graphene composite aerogel. The composite electrode showed a great specific capacitance (721 F g^{-1} at 1 A g^{-1}), a capacitance retention rate (89.2% at 20 A g^{-1}) and an instantaneous cycle stability of 92.3% at 10 A g^{-1} after 10,000 cycles [66]. Electrode materials based on carbon quantum dots (CQDs) have received more and more attention due to their many unique characteristics. The CQD is prepared by changing the chemical oxidation method for developing a new type of three-dimensional N,P co-doped CQD/reduced graphene oxide (rGO) composite aerogels (N,P-CQDs/rGO). Compared with GO, rGO, N, P-rGO and CQDs/rGO, the specific capacitance of N,P-CQDs/rGO is significantly improved (453.7 F g^{-1} at 1 A g^{-1}). In addition, the synthesized N,P-CQD/rGO has excellent rate characteristics (capacitance retention rate at 50 A g^{-1} is 69.5%). In expansion, the symmetrical device is based on the N,P-CQDs/rGO composite aerogel, which accomplishes a high energy density of of 15.69 Wh kg^{-1} at a power density of 325 W kg^{-1} [67].

Wei *et al*. [68] used a simple one-step hydrothermal route and the subsequent calcination method to effectively prepare CQDs/$NiCo_2O_4$ nanocomposites with different morphologies. They show high specific capacitances, superior rate performances and high cycling stabilities. A simple one-step solvothermal process has been used to prepare the double hydroxide (LDH) composite material. The formed porous CQDs/NiAl-LDH composite showed an expanded specific surface area and nanoscale size. The composite displayed great electrochemical performance with high rate capability of 967 F g^{-1} at 20 A g^{-1}, superior specific capacitance of 1794 F g^{-1} and great cycle stability around 93% retention over 1500 cycles [69].

Porous carbon: An important type of porous carbons, which is broadly utilized in activated carbons [70]. Activated carbon is more often than not induced from charcoal and utilized in air purification, gold purification, metal extraction, solvent recovery, water purification, medication, methane and hydrogen storage, drain treatment, filters in compressed and respirators, teeth brightening, hydrogen chloride generation and numerous other applications [71]. Porous carbon is widely regarded as a double layer capacitor due to its good chemical stability, high surface area, simple processability and long cycle life [72]. Very porous carbon materials can be arranged through evaporative drying and thermochemical treatment of resorcinol-formaldehyde gels [73-75]. Electrodes for supercapacitors were prepared by Chen *et al*. [76] through settle down of PANI on carbons with large surface area. The energy storage properties of the capacitors were examined using electrodes in 1 M H_2SO_4 at constant current charge-discharge cycles within a potential extend from 0 to 0.6 V. The specific capacitance of polyaniline based electrode and bare-carbon electrode were found to be 180 and 92 F g^{-1}, respectively. Yu *et al.* [77] developed nitrogen-doped porous carbon nanofibers based electrode material through carbonization of macroscopic carbon nanofibers (CNFs) treated with polypyrrole at suitable conditions. The reversible specific capacitance of composite nanofibers is measured to be 202.0 F g^{-1} in 6 M aqueous KOH electrolyte at the current density of 1.0 A g^{-1}, meantime maximum power density of 89.57 kW kg^{-1} and capacitance retention capability were maintained.

A simple chemical activation method was used to synthesis three-dimensional hierarchical porous carbon (THPC) using KOH as the activator and polypyrrole sheets as the precursor [78]. The specific surface area, specific capacitance and electrical conductivity were found to be 2870 m^2 g^{-1}, 189.0 F g^{-1} and 5.6 S cm^{-1}, respectively. This unique function makes THPC a perfect electrodes for supercapacitors. Moreover, the THPC shows high capacity, superior rate capability and long cycle life. In another work [79], nitrogen-doped porous carbon was developed by the carbonization of urea-formaldehyde resins (UF) and calcium acetate monohydrate. The UF-Ca-700-3:1 test shows specific capacitances of 334.8 F g^{-1} and 224.0 F g^{-1} in 6M KOH, at the current density of 0.5 and 1.0 A g^{-1} individually. At the current densities of 20 and 40 A g^{-1}, the UF-Ca-900-3:1 shows high specific capacitance retention of 67.1% and 51.4%, separately. Thus, the nitrogen-doped carbon shows an excellent electrode material for supercapacitors, which would be widely connected for industrial applications [79]. Boron and nitrogen co-doped porous carbons (BNCs) were prepared by Guo & Gao [80] using a simple synthetic route by using citric acid, boric acid and nitrogen as C, B and N precursors, separately. Electrochemical properties of cell were analyzed using cyclic voltammetry and galvanostatic charge/discharge tests. The BNC-9 and BNC-15 tests with specific surface areas of 894 and 726 m^2 g^{-1} appeared the specific capacitance up to 268 and 173 F g^{-1}, individually, with the current of 0.1 A g^{-1}. At current density 0.1 A g^{-1}, the power densities of 165 and 201 W kg^{-1} and the energy densities of 3.8 and 3.0 Wh kg^{-1} were measured for BNC-9 and BNC-15, separately. Hence, BNC-15 is more appropriate to apply in power storage requirements, whereas BNC-9 has tendency to store more energy [80]. Wang *et al.* [81] presented a facile method to synthesize 3D flower-like and hierarchical porous carbon (FHPC) materials utilizing ZnO as the template followed by KOH activation. This framework contains various micropores and well-defined mesopores within the interconnected macroporous walls. The FHPC electrode can accomplish high capacitance of 294 F g^{-1} at a scan rate of 2 mV s^{-1} and great rate capability with superior

cycle in 6 M KOH electrolyte. The symmetric supercapacitor manufactured with FHPC electrodes conveys energy density of 15.9 Wh kg^{-1} and power density of 317.5 W kg^{-1} worked within the voltage range of 0-1.8 V in 1 M Na_2SO_4 electrolyte. Thus, FHPC can be an exceedingly excellent electrode material for high energy storage supercapacitors. Liu *et al.* [82] synthesized MnO_2/PC microspheres with a fractional graphitic structure for high supercapacitor performance. Carbon microspheres with micro/mesoporous were prepared by hydrothermal emulsion polymerization and activation process. Manganese nitrate was encapsulated into the porus carbon (PC) microspheres. Consequent thermal treatment drives the formation of amorphous MnO_2. The resulting MnO_2/PC microsphere electrodes appeared a great electrochemical specific capacitance (459 F g^{-1} at 1.0 A g^{-1}) and great rate capability (77% retention at 20.0 A g^{-1}). The electrode materials in the electrochemical double-layer capacitors with their specific properties are shown in Table-1.

Pseudocapacitors: Energy is stored by pseudocapacitors *via* the reversible faradaic charge exchange, which requires a rapid and reversible electrochemical redox reaction at the anode-electrolyte interface [83]. Pseudocapacitors are part of electrochemical capacitors, combined with electric double layer capacitors (EDLC) to form supercapacitors [84]. When a potential is applied to the capacitor, the electrode material is reduced and oxidized, including the charge into the double layer, which is caused by the Faradic current of the supercapacitor battery [85]. A high surface area and high electrical conductivity are basic for the high-performance electrodes because the eletrochemical redox reactions take place on the electrode surface. Hence, carbon nanomaterials such as graphene, CNTs, mesoporous carbon and their hybrids, have moreover been utilized as the substrate for loading active materials and current collectors to make sure high capacitance and quick charge transfer for electrodes in high-performance pseudocapacitors [86]. Compared to EDLCs, the Faradic reaction included in the pseudocapacitors helps to attain high specific capacitance and energy densities [87]. Pseudocapacitors endure from a relatively lower power density and need of cycling stability when compared with EDLCs. The most widely used pseudocapacitive materials are metal oxides and electronically conducting polymers including polyanilines, polypyrroles and polythiophenes.

Metal oxides: Several transition metal oxides *e.g.* Cu, Fe, Ni, Mn, Cu and Ru oxides, provide a rich redox reactions for the electrode materials. For example, in electrochemical cells, they provide high specific capacitance values for supercapacitors. Ruthenium oxide (RuO_2) could be an eminent material showing high particular capacitance and great reversibility [88]. Currently, CuO-based supercapacitors have recently attracted significant consideration due to promising capacitance, naturally friendliness, great electrochemical execution and lower cost. Singu *et al.* [89] developed a β-$Ni(OH)_2$ nanodiscs by chemical precipitation and used as supercapacitors. The β-$Ni(OH)_2$ nanodiscs showed specific capacitance of 400 F g^{-1}, energy density of 7.15 W h kg^{-1} and power density of 1716 W kg^{-1} at the current thickness of 1 A g^{-1}. Obodo *et al.* [90] reported that the three-dimensional (3D) nickel froth could be a promising electrode material for storing energy in different gadgets since they have expanded surface area, exceptionally conductive and appreciate a continuous penetrable 3D system. Hence, the 3D nickel foam-based electrodes with metal oxides/

TABLE-1
ELECTRODE MATERIALS IN ELECTROCHEMICAL DOUBLE-LAYER CAPACITORS

Electrode materials	Electrolyte	Specific capacitance	Power density	Energy density	Retention capability	Ref.
(i) Carbon nanotube (CNT) based materials						
SWNT	1 M Et_4NBF_4/propylene carbonate	160 F g^{-1} at 4V	24 kW kg^{-1}	17 Wh kg^{-1}	96.4% after 1000 cycles	[37]
MWCNT	6 mol/l KOH	80–135 F g^{-1}	–	–	–	[37]
(ii) Graphene based materials						
Graphene sheets	30 wt.% KOH in H_2O	550 F g^{-1}	136 W kg^{-1} at 1A g^{-1}	85.6 Wh kg^{-1}	–	[46]
MnO_2 nanowire/graphene	Neutral aqueous Na_2SO_4	–	5000 W kg^{-1}	7.0 Wh kg^{-1}	–	[48]
Graphene nanoplate-MnO_2	1 M Na_2SO_4	308.5 F g^{-1}	–	–	–	[49]
GO/MnO_2 nanowires	1 M Na_2SO_4	360.3 F g^{-1}	–	–	93% after 1000 cycles	[50]
(iii) Carbon quantumdots (CQDs)						
CQDs/PPy composite	1.0 M KCl	308 F g^{-1}	–	–	85.7% after 2000 cycles	[61]
CQDs/$NiCo_2O_4$ composite	2 M KOH	856 F g^{-1}	128 W kg^{-1}	13.1 Wh kg^{-1}	101.9% after 5000 cycles	[62]
N, P-CQDs/rGO	6 M KOH	453.7 F g^{-1}	325 W kg^{-1}	15.69 Wh kg^{-1}	93.5% after 10000 cycles	[67]
(iv) Porous carbon						
PANI/PC	1 M H_2SO_4	180 F g^{-1}	–	–	–	[76]
N-CNFs electrode	1 M KOH	202 F g^{-1}	89.57 kW kg^{-1}	–	97% after 3000 cycles	[77]
BNC	6 M KOH	268 F g^{-1}	165 W kg^{-1}	3.8 Wh kg^{-1}	–	[80]
FHPC electrode	6 M KOH	294 F g^{-1}	317.5 W kg^{-1}	15.9 Wh kg^{-1}	71% after 5000 cycles	[81]

hydroxides of distinctive morphologies are also applied for high-performance pseudocapacitors. A novel 3D reduced graphene oxide aerogel and MnO_2 (rGO/MnO_2) hybrid was prepared by Zhao *et al*. [91] through a mild method and freeze-drying treatment, followed by an electrodeposition process. The rGO/MnO_2 on Ni froth showed specific capacitance of 288 F g^{-1} at 0.5 A g^{-1}. It was found that the stored MnO_2 is uniformly bound to the graphene sheet used to produce high-performance supercapacitors as a binder-free electrode material [91].

Conducting polymers: Conductive polymers, namely polypyrrole (PPy), polyaniline (PANI), polythiophene (PTh) and their comparative derivatives, provide pseudocapacitive behaviour through redox reactions [92]. Various conductive polymers can be widely required as electrode materials for supercapacitors because of its easy synthesis and low cost [93]. In comparison with carbon electrode materials, conducting polymers have a generally high conductivity and high capacitance [94]. Conductive polymer is an organic polymer, which can conduct energy along the polymer chain through the conjugated system [95]. Until recently, conductive polymers have been regarded as one of the most excellent electrode materials for flexible supercapacitors because of their good flexibility and easy synthesis [96]. Greater surface area and greater porosity nanostructured conductive polymers have excellent conduction pathways, surface interactions and long surface-to-volume commitment in nanoscale dimensions, so they can be used for large-scale demonstrations [97].

Polyaniline: Recently, polyaniline is stored in a flexible current collector used for pseudocapacitor applications using spray technology. By utilizing the spraying method, PANI is followed and consistently disseminated along the surface of the current collector. The electrochemical characteristics of PANI expose a superior capacitive efficiency. A high specific capacitance of 594.92 F g^{-1} was found at a scan rate of 5 mV s^{-1}. The results exhibit an increment in the energy density of 82.63 Wh kg^{-1} at a potential difference of 1 V in the presence of 4 M KOH aqueous electrolyte [98]. Sivakkumar *et al*. [99] prepared polyaniline (PANI) nanofibres by interfacial polymerization and assessed their electrochemical execution in an aqueous redox supercapacitor constitutes a two-electrode battery. At a constant current of 1.0 A g^{-1}, the initial specific capacitance of the battery is 554 F g^{-1}, but on continuous cycling, this value diminishes quickly. In arrange to develop cycling ability of the supercapacitor, a polyaniline composite with multi-walled carbon nanotubes (MWCNTs) was prepared by *in situ* chemical polymerization. Li *et al.* [100] evaluated the theoretical mass specific capacitance of polyaniline by combining electric double layer capacitance and pseudo capacitance. The most extreme specific capacitance was 2.0×10^3 F g^{-1} for one single PANI electrode. In this work, the most extreme specific capacitance values measured by CV, EIS and galvanostatic charge/discharge methods are 608, 445.0 and 524.9 F g^{-1}, individually. The experimental value is much smaller than the theoretical value. Homogeneous PANI nanofibers with a wide surface area (low diameter and rough surface) should be connected to change the substrate in order to promote the production of supercapacitors.

Polypyrrole: Polypyrrole is a prominent conducting polymer, which has been widely used in supercapacitors [101]. Polypyrrole has been broadly considered for biomedical and industrial applications [102]. Polypyrrole was effectively electropolymerized on pre-passivated Fe electrode in an aqueous solution containing monomer and oxalic acid. Polypyrrole coated Fe electrode may be a promising novel material with electrochemical properties acquired by cyclic voltammetry, galvanostatic charge-discharge cycling test, EIS and other electrochemical techniques. This electrode has a few vital advantageous as a supercapacitor such as reasonable, easy to synthesis, soundness, lightweight, long cycle life, high specific capacitance values and no corrosion risk in application [103]. Jiao *et al*. [104] synthesized a simple and cost-effective interfacial polymerization method to plan large-area flexible transparent PPy/PET films for manufacturing a low-haze transparent supercapacitors. This film has a high consistency with a small radius of curvature of 0.8 mm still has good conductivity retention under twisting and has high clarity when the haze is low (1.40 %). Graphene sheets coated with MnO_x particles and polypyrrole overlap each other to form a 3D conducting network that improved the connection between the electrode material and the electrolyte and which acted as spacers to maintain the detachment of neighboring sheets [101]. Rajesh *et al*. [105] reported on the electropolymerization of phytic corrosive (PA) doped polypyrrole thin film for supercapacitor application. The films appeared an excellent supercapacitive performance in both stainless steel and titanium substrates. The PA/PPy electrodes displayed high charge/discharge efficiency and better capacitance maintenance.

Polythiophene: Polythiophene and its derivatives can be p- and n-type conducting polymers [106]. In common, polythiophene tends to have low conductivity but the *p*-doped polymers are exceptionally stable in air. Compared with PANI and polypyrrole, the specific capacitance of polythiophene-based electrodes is usually lower, but the main advantage is that it can work in a relatively high potential window (~1.2 V) [97]. Laforgue *et al.* [107] chemically synthesized polythiophene and poly(*p*-fluorophenylthiophene) (PFPT) for utilize as active materials in supercapacitor electrodes. Specific capacitance values of 7 mAh g^{-1} and 40 mAh g^{-1} were measured for PFPT and polythiophene, individually. Polythiophene was electrochemically polymerized by a galvanostatic process in an oil-in-ion fluid microemulsion on multiwalled carbon nanotube (MWCNT) improved carbon paper. The prepared polythiophene/MWCNT composite had an interlaced system morphology, in which polythiophene with a thickness of 2-3 nm was consistently layered by the MWCNTs. The results showed that the composite film had a desirable capacitance with a great electron transfer rate and lower resistance. It also showed great cycle stability after 500 cycles, with a low rate of specific capacitance. The results demonstrated the possibility of the developed polythiophene/MWCNT composite can be utilized as an electrode material for supercapacitors [108]. The electrode materials in pseudocapacitors with their specific properties are shown in Table-2.

Hybrid capacitors: Hybrid system offers a combination of EDLS and perovskites solar cells (PSCs), that's by combining

TABLE-2
ELECTRODE MATERIALS IN PSEUDOCAPACITORS

Electrode materials	Electrolyte	Specific capacitance	Power density	Energy density	Retention capability	Ref.
(i) Metal oxides based materials						
β-$Ni(OH)_2$ nanodiscs	1 M aqueous KOH	400 F g^{-1}	1716 W kg^{-1}	7.15 Wh kg^{-1}	83% after 1500 cycles	[89]
3D-nickel foam	Oxidative alkaline solution	2384.3 F g^{-1}	–	–	75% after 3000 cycles	[90]
rGO/MnO_2	10 mM Na_2SO_4, 0.1 M $Mn(CH_3COO)_2$	288 F g^{-1}	8.61 kW kg^{-1}	26.82 Wh kg^{-1}	94.7% after 1000 cycles	[91]
(ii) Conducting polymers (CPs) based materials						
PANI based materials						
PANI/CSA	4 M aqueous KOH	594.92 F g^{-1}	–	82.63 Wh kg^{-1}	–	[98]
PANI nanofibres	1.0 M H_2SO_4	554 F g^{-1}	–	–	–	[99]
PANI/SS	1.0 M H_2SO_4	2.0×10^3 F g^{-1}	–	–	–	[100]
PPy based materials						
Fe/PPy	0.3 M $H_2C_2O_4$	2280 F g^{-1}	–	–	–	[103]
PPy/PET	1 M H_3PO_4	1.64 mF cm^{-2}	67.3 mWh cm^{-3}	5 mWh cm^{-3}	80% after 1000 cycles	[104]
PA/PPy/SS	1 M H_2SO_4	297 F g^{-1}	41.25 Wh kg^{-1}	–	–	[105]
PTh/MWCNT	1 mol L^{-1} Na_2SO_4	216 F g^{-1}	–	–	–	[108]

the energy source of battery-like electrode and capacitor-like electrode within the same cell [109]. Hybrid capacitors have accomplished energy and power densities more prominent than EDLCs without the sacrifices in cycling stability. Here hybrid utilizes both Faradaic and non-Faradaic processes to store charge [110]. They have an excellent cycle life and more than 20,000 charge/discharge cycles can be envisaged, instead of the battery delivering hundreds or thousands of charge/discharge [111]. These capacitors store charge at the surface of the electrodes rather than inside the electrodes as batteries do. Hybrid capacitors mainly utilized for a few applications, such as: Spotlights, LED applications, communications, memory back-up, onboard chargers, solar charge applications, motor inverters [112]. Based on electrode configuration, it can be classified into three types: composite, asymmetric and battery-type.

Composite hybrid: Composite hybrids are developed from carbon based materials with incorporated pseudocapacitive materials such as conducting polymers and metal oxides (Fig. 3) [34,113]. Carbon nanotubes provide the backbone for the uniform distribution of metal oxides or conductive polymers (ECP), resulting in excellent pseudo capacitance and double-layer capacitance [114]. Such electrodes are more capable than either pure carbon or pure metal oxide or polymer electrodes [31]. Saikia *et al.* [115] described the manufacturing process of supercapacitor electrodes of carboxylic acid-functionalized carbon nanotube/graphene composite (rGO/FCNT) without destroying the 2D flake structure of reduced graphene oxide flakes. By treating with a mixture of H_2SO_4/HNO_3, the carboxyl functional groups are presented on the surface of the carbon nanotubes. The material appears a specific capacitance of 302 F g^{-1} at a current thickness of 1 A g^{-1} [115]. In other work, nickel-inserted zeolite-imidazolate framework/graphene (ZIF-67/rGO) has brought excellent electrochemical properties by inducing additional pseudocapacitance [116]. This electrode material accomplished high specific capacitance of 304 F g^{-1} at a current density of 1 A g^{-1} in the presence of 1 M H_2SO_4 as an aqueous electrolyte. An effortless pulsed electrochemical method is created for the arrangement of permeable reduced graphene oxide/polypyrrole (rGO/PPy) composite films. This strategy combines blade casting of graphene oxide gel and pulse electrochemical technology, which not only simplifies the precursor electrolyte but moreover preserves the permeable structure of

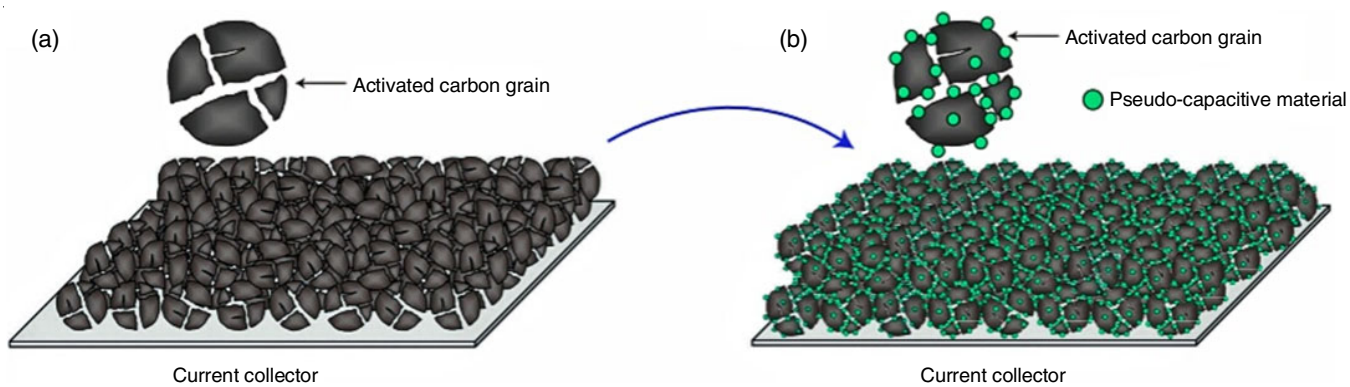

Fig. 3. To improve both energy and power densities for electrochemical capacitors. a & b, Decorating activated carbon grains (a) with pseudo-capacitive materials (b) [Ref. 34]

graphene oxide gel. Composite shows a well-defined permeable structure, driving to specific capacitance of 414 F g^{-1} at 0.2 mA cm^{-2} [117]. Deng *et al*. [118] synthesized sponge-like carbon foam and nanostructured δ-MnO_2 composite materials not only provide large exposed electroactive surface area, but also provide the fast electron and ion transport paths benefit from the 3D interconnected layered permeable surface and the large number of open channels between the anchored MnO_2 sheets. Inspite of the fact that the resultant composite exhibited capacitance of 146 F g^{-1} and an impressive energy density of 20.3 Wh kg^{-1} at 1 A g^{-1} with great cycling stability in 6 M KOH electrolyte. Yadav *et al*. [119] reported the synthesis of polypyrrole-doped nickel oxide multi-walled carbon nanotube composites, which created many active sites for ion migration reactions, thereby promoting energy storage mechanisms. Composite was considered as an electrode material in supercapacitor and displayed specific capacitance of 395 F g^{-1} and cyclic stability up to 5000 cycles at 0.5 A g^{-1}.

Asymmetric hybrid: Asymmetric hybrids combine Faradaic and non-Faradaic processes by coupling an EDLC electrode with a pseudocapacitor electrode [120] It is constructed by using carbon material as the negative terminal and metal oxide or conductive polymer as the positive terminal [121]. Liu *et al.* [122] synthesized the MnO_2/$MnCO_3$/graphene aerogels (MGA) by shape-controlled rod-like MnO_2 and the incorporation of reduced graphene oxide (rGO) into the granular $MnCO_3$ hybrid nanostructure. Asymmetric supercapacitors were created utilizing MGA as the positive electrode and rGO aerogel as the negative terminal in a neutral aqueous Na_2SO_4 electrolyte. The asymmetric supercapacitor shows an energy density of 17.8 W h kg^{-1} [122]. Chen *et al.* [123] have fabricated transition-metal-oxide nanowire/single-walled carbon nanotube (SWNT) hybrid thin-film terminals-based asymmetric supercapacitors. It shows mechanical adaptability, uniform layered structures and mesoporous surface morp-hology. Here, indium oxide nanowire/SWNT hybrid film was used as the negative terminal and the MnO_2 nanowire/SWNT hybrid film was used as the positive terminal. It seems to dominate the device with a specific capacitance and energy density are 184 F g^{-1} and 25.5 Wh kg^{-1}, respectively. A high-performance supercapacitors with cycling stabiltiy dependent on the special core-shell structure and well-designed combinations was designed by $NiCO_2S_4$/NiO core-shell nanowire clusters (NWAs). The NWAs as the positive terminal and dynamic carbon as the negative anode, conveying a high energy density found to be 30.38 W h kg^{-1} at 0.288 kW kg^{-1} [124]. Zhou *et al.* [125] have prepared asymmetric supercapacitor by using bamboo-like nanomaterial composed of V_2O_5/polyindole (V_2O_5/PIn) decorated onto the enacted carbon cloth was manufactured for supercapacitors. The polyindole seems successfully improve the electronic conductivity and avoid the dissolution of vanadium and it has high specific capacitance of 535.5 F g^{-1} and high energy density 38.7 W h kg^{-1} at a power density of 900 W kg^{-1}.

Battery type hybrid: Battery type supercapacitor coordinating a battery type electrode with a capacitor type electrode [126]. Fundamentally, the positive electrode stores charge like a battery, while the carbon negative electrode stores charge like an electrochemical capacitor [127]. This may give both the advantages of a battery (higher energy) and a capacitor (higher rate and control). The highly conductive and reactive Ag_2S layer simplifies the diffusion of electrolyte ions to approach the active Cu_2S material and promotes rapid electron transport, thereby realizing high-performance battery-type supercapacitors. The Cu_2S single bond Ag_2S composite electrode displayed high specific capacity of 772 C g^{-1} at a filter rate of 10 mV s^{-1} [128]. A hybrid supercapacitor was assembled with bundle like $CuCo_2O_4$ microstructures as the cathode and activated carbon as the anode, which shown specific capacity of 152.25 C g^{-1} at 1 A g^{-1} and energy density of 39.95 W h kg^{-1} at 944.63 W kg^{-1} [129]. Li *et al*. [130] have been detailed battery hybrid supercapacitor based on a carbon skeleton/Mg_2Ni independent electrode, which exhibited good specific capacities of 296 F g^{-1} and greater discharge capacity of 644 mAh g^{-1}. The hybrid system can switch between battery and supercapacitor modes quickly as required during application. A layered vanadium(IV) oxide used as an anode on the heterostructure of reduced graphene oxide (rGO/VO_2) and enacted carbon on carbon cloth as a cathode are proposed for manufacturing an progressed battery type supercapacitors. The mixed valence of vanadium particles in the prepared VO_2 network (V^{3+} and V^{4+}) promotes the redox reaction at low potential, which leads to rGO/VO_2 as a normal anode. It yields a high specific capacity of 1214 mAh g^{-1} at 0.1 A g^{-1} after 120 cycles, with a high rate capability and stability [131]. The electrode materials in hybrid capacitors with their specific properties are shown in Table-3.

Conclusion

Compared with batteries, supercapacitors have great power density, shorter charging time, great discharge/charge cycle stability and broad temperature range applicability. These points of interest create supercapacitors valuable for different potential applications, such as wind turbines, renewable-energy-storage devices and automoblies. In this review, the most broadly used electrode materials for designing various types of supercapacitors and their characteristic performance are focussed. Compared with electrochemical double-layer capacitors, conductive polymers and metal oxide materials both increase specific capacitance due to the Faradaic charge exchange. The disadvantages of polymer and metal oxide such as lower cycle stability and lower power density, which can be solved by combining them with carbon based materials to form composite, which also leads to increase in conductivity and thickness of electrode. Among conducting polymers, polyaniline shows high specific capacitance due to excellent proton activity in the electrolyte. In hybrid capacitors, carbon materials provide the backbone for the uniform distribution of metal oxides or conductive polymers, resulting in greater energy density and longer cycle life. Hybrid capacitors have both battery and super capacitor characteristics, which eliminates the limitations of other types of supercapacitors. When manufacturing high-performance supercapacitors, in addition to power density, energy density, cycle stability and other factors, we should also pay attention to factors such as cost, environmental impact and resource availability.

TABLE-3
ELECTRODE MATERIALS IN HYBRID CAPACITORS

Electrode materials	Electrolyte	Specific capacitance	Power density	Energy density	Retention capability	Ref.
(i) Composite materials						
rGO/FCNT	1 M H_2SO_4/HNO_3	302 F g^{-1}	–	–	–	[115]
ZIF-67/rGO	1M H_2SO_4	304 F g^{-1}	1 kW kg^{-1}	21.5 Wh kg^{-1}	87% after 4500 cycles	[116]
WFCF/MnO_2-2.0	6 M KOH	46 F g^{-1}	2282 W kg^{-1}	20.3 Wh kg^{-1}	70% after 5000 cycles	[118]
NiO@NMWCNT/PPy	2 M KOH	395 F g^{-1}	–	–	90% after 5000 cycles	[119]
(ii) Asymmetric						
MnO_2/$MnCO_3$/rGO	1 M Na_2SO_4	–	400 W kg^{-1}	17.8 Wh kg^{-1}	–	[122]
Metal-oxide/SWNT	1 M Na_2SO_4	184 F g^{-1}	50.3 kW kg^{-1}	25.5 Wh kg^{-1}	–	[123]
$NiCo_2S_4$@NiO/NWAs	3 M KOH	12.2 F cm^{-2}	0.288 kW kg^{-1}	30.38 Wh kg^{-1}	109% after 5000 cycles	[124]
V_2O_5/Pin	5 M $LiNO_3$	535.5 F g^{-1}	900 W kg^{-1}	38.7 Wh kg^{-1}	91.1% after 5000 cycles	[125]
(iii) Battery type						
Cu_2S - Ag_2S metal sulphide	3 M KOH	772 C g^{-1}	–	0.251 k Wh kg^{-1}	89% after 2000 cycles	[128]
$CuCo_2O_4$ BMs	2 M KOH	303.22 C g^{-1}	944.63 W kg^{-1}	39.95 Wh kg^{-1}	71.8% after 5000 cycles	[129]
rGO/MWCNTs	6 mol/L KOH	296 F g^{-1}	–	–	100% after 100 cycles	[130]
rGO@VO_2	1 M $LiPF_6$	1214 mAh g^{-1}	10000 W kg^{-1}	126.7 Wh kg^{-1}	–	[131]

ACKNOWLEDGEMENTS

The authors (ASN, VJ and VJ) would like to thank and acknowledge Karunya Institute of Technology and Sciences for providing necessary facilities to initiate 'Supercapacitors based research activity' in the Department of Applied Chemistry.

CONFLICT OF INTEREST

The authors declare that there is no conflict of interests regarding the publication of this article.

REFERENCES

1. P.J. Hall and E.J. Bain, *Energy Policy*, **36**, 4352 (2008); https://doi.org/10.1016/j.enpol.2008.09.037
2. B. Zhao, D. Chen, X. Xiong, B. Song, R. Hu, Q. Zhang, B.H. Rainwater, G.H. Waller, D. Zhen, Y. Ding, Y. Chen, C. Qu, D. Dang, C.-P. Wong and M. Liu, *Energy Storage Mater.*, **7**, 32 (2017); https://doi.org/10.1016/j.ensm.2016.11.010
3. S. Liu, L. Wei and H. Wang, *Appl. Energy*, **278**, 115436 (2020); https://doi.org/10.1016/j.apenergy.2020.115436
4. J.R. Miller and P. Simon, *Science*, **321**, 651 (2008); https://doi.org/10.1126/science.1158736
5. E. Frackowiak and F. Beguin, *Carbon*, **39**, 937 (2001); https://doi.org/10.1016/S0008-6223(00)00183-4
6. R. Kotz and M. Carlen, *Electrochim. Acta*, **45**, 2483 (2000); https://doi.org/10.1016/S0013-4686(00)00354-6
7. Y. Jiang and J. Liu, *Energy, Environ. Mater.*, **2**, 30 (2019); https://doi.org/10.1002/eem2.12028
8. M.J. Young, A.M. Holder, S.M. George and C.B. Musgrave, *Chem. Mater.*, **27**, 1172 (2015); https://doi.org/10.1021/cm503544e
9. Y. Li, M. van Zijll, S. Chiang and N. Pan, *J. Power Sources*, **196**, 6003 (2011); https://doi.org/10.1016/j.jpowsour.2011.02.092
10. D. Majumdar, M. Mandal and S.K. Bhattacharya, *Emergent Mater.*, **3**, 347 (2020); https://doi.org/10.1007/s42247-020-00090-5
11. B. Xu, S. Yue, Z. Sui, X. Zhang, S. Hou, G. Cao and Y. Yang, *Energy Environ. Sci.*, **4**, 2826 (2011); https://doi.org/10.1039/c1ee01198g
12. P. Sharma and T.S. Bhatti, *Energy Convers. Manage.*, **51**, 2901 (2010); https://doi.org/10.1016/j.enconman.2010.06.031
13. T.K. Enock, C.K. King'ondu, A. Pogrebnoi and Y.A.C. Jande, *Int. J. Electrochem.*, **2017**, 6453420 (2017); https://doi.org/10.1155/2017/6453420
14. L.L. Zhang, R. Zhou and X.S. Zhao, *J. Mater. Chem.*, **20**, 5983 (2010); https://doi.org/10.1039/c000417k
15. H. Xian, T. Peng, H. Sun and J. Wang, *J. Mater. Sci.*, **50**, 4025 (2015); https://doi.org/10.1007/s10853-015-8959-3
16. N.L. Wu, *Mater. Chem. Phys.*, **75**, 6 (2002); https://doi.org/10.1016/S0254-0584(02)00022-6
17. M. Hasan and M. Lee, *Progress Nat. Sci: Mater. Int.*, **24**, 579 (2014); https://doi.org/10.1016/j.pnsc.2014.10.004
18. C. Huang, J. Zhang, N.P. Young, H.J. Snaith and P.S. Grant, *Sci. Rep.*, **6**, 25684 (2016); https://doi.org/10.1038/srep25684
19. T. Esawy, M. Khairy, A. Hany and M.A. Mousa, *Appl. Phys., A Mater. Sci. Process.*, **124**, 566 (2018); https://doi.org/10.1007/s00339-018-1967-9
20. W. Chen, R.B. Rakhi, L. Hu, X. Xie, Y. Cui and H.N. Alshareef, *Nano Lett.*, **11**, 5165 (2011); https://doi.org/10.1021/nl2023433
21. L. Caizán-Juanarena, C. Borsje, T. Sleutels, D. Yntema, C. Santoro, I. Ieropoulos, F. Soavi and A. ter Heijne, *Biotechnol. Adv.*, **39**, 107456 (2020); https://doi.org/10.1016/j.biotechadv.2019.107456
22. Z.S. Iro, C. Subramani and S.S. Dash, *Int. J. Electrochem. Sci.*, **11**, 10628 (2016); https://doi.org/10.20964/2016.12.50
23. O.S. Okwundu, C.O. Ugwuoke and C.O. Augustine, *Metall. Mater. Trans., A Phys. Metall. Mater. Sci.*, **25**, 105 (2019); https://doi.org/10.30544/417
24. J.R. Rani, R. Thangavel, S.I. Oh, S.Y. Lee and J.H. Jang, *Nanomaterials*, **9**, 148 (2019); https://doi.org/10.3390/nano9020148
25. X. Li and B. Wei, *Nano Energy*, **2**, 159 (2013); https://doi.org/10.1016/j.nanoen.2012.09.008

26. P. Ratajczak, M.E. Suss, F. Kaasik and F. Béguin, *Energy Storage Mater.*, **16**, 126 (2019); https://doi.org/10.1016/j.ensm.2018.04.031
27. Z. Zhou, Y. Zhu, Z. Wu, F. Lu, M. Jing and X. Ji, *RSC Adv.*, **4**, 6927 (2014); https://doi.org/10.1039/c3ra46641h
28. M. Jayalakshmi and K. Balasubramanian, *Int. J. Electrochem. Sci.*, **3**, 1196 (2008).
29. P. Sharma and V. Kumar, *Pramana Res. J.*, **8**, 50 (2018).
30. R.S. Kate, S.A. Khalate and R.J. Deokate, *J. Alloys Compd.*, **734**, 89 (2018); https://doi.org/10.1016/j.jallcom.2017.10.262
31. K. Krishnan, P. Jayaraman, S. Balasubramanian and U. Mani, *J. Mater. Chem. A Mater. Energy Sustain.*, **6**, 23650 (2018); https://doi.org/10.1039/C8TA09524H
32. A. Muzaffar, M.B. Ahamed, K. Deshmukh and J. Thirumalai, *Renew. Sustain. Energy Rev.*, **101**, 123 (2019); https://doi.org/10.1016/j.rser.2018.10.026
33. E. Redondo, L.W.L. Fevre, R. Fields, R. Todd, A.J. Forsyth and R.A.W. Dryfe, *Electrochim. Acta*, **360**, 136957 (2020); https://doi.org/10.1016/j.electacta.2020.136957
34. P. Simon and Y. Gogotsi, *Nat. Mater.*, **7**, 845 (2008); https://doi.org/10.1038/nmat2297
35. O. Erol, I. Uyan, M. Hatip, C. Yilmaz, A.B. Tekinay and M.O. Guler, *Nanomedicine*, **14**, 2433 (2018); https://doi.org/10.1016/j.nano.2017.03.021
36. A. Venkataraman, E.V. Amadi, Y. Chen and C. Papadopoulos, *Nanoscale Res. Lett.*, **14**, 220 (2019); https://doi.org/10.1186/s11671-019-3046-3
37. X. Chen, R. Paul and L. Dai, *Natl. Sci. Rev.*, **4**, 453 (2017); https://doi.org/10.1093/nsr/nwx009
38. A.K. Geim and K.S. Novoselov, *Nat. Mater.*, **6**, 183 (2007); https://doi.org/10.1038/nmat1849
39. D.G. Papageorgiou, I.A. Kinloch and R.J. Young, *Prog. Mater. Sci.*, **90**, 75 (2017); https://doi.org/10.1016/j.pmatsci.2017.07.004
40. N.M.R. Peres and R.M. Ribeiro, *New J. Phys.*, **11**, 095002 (2009); https://doi.org/10.1088/1367-2630/11/9/095002
41. R.R. Nair, P. Blake, A.N. Grigorenko, K.S. Novoselov, T.J. Booth, T. Stauber, N.M.R. Peres and A.K. Geim, *Science*, **320**, 1308 (2008); https://doi.org/10.1126/science.1156965
42. S. Zhu, S. Yuan and G.C.A.M. Janssen, *Europhys. Lett.*, **108**, 17007 (2014); https://doi.org/10.1209/0295-5075/108/17007
43. W. Kong, H. Kum, S.-H. Bae, J. Shim, H. Kim, L. Kong, Y. Meng, K. Wang, C. Kim and J. Kim, *Nat. Nanotechnol.*, **14**, 927 (2019); https://doi.org/10.1038/s41565-019-0555-2
44. M.I. Bhavana and H.J. Ahalapatiya, *Chem. Sci. Int. J.*, **23**, 1 (2018); https://doi.org/10.9734/CSJI/2018/41031
45. R. Karthick and F. Chen, *Carbon*, **150**, 292 (2019); https://doi.org/10.1016/j.carbon.2019.05.017
46. C. Liu, Z. Yu, D. Neff, A. Zhamu and B.Z. Jang, *Nano Lett.*, **10**, 4863 (2010); https://doi.org/10.1021/nl102661q
47. H. Yang, S. Kannappan, A.S. Pandian, J.-H. Jang, Y.S. Lee and W. Lu, *Nanotechnology*, **28**, 445401 (2017); https://doi.org/10.1088/1361-6528/aa8948
48. Z.-S. Wu, W. Ren, D.-W. Wang, F. Li, B. Liu and H.-M. Cheng, *ACS Nano*, **4**, 5835 (2010); https://doi.org/10.1021/nn101754k
49. H. Huang and X. Wang, *Nanoscale*, **3**, 3185 (2011); https://doi.org/10.1039/c1nr10229j
50. K. Dai, L. Lu, C. Liang, J. Dai, Q. Liu, Y. Zhang, G. Zhu and Z. Liu, *Electrochim. Acta*, **116**, 111 (2014); https://doi.org/10.1016/j.electacta.2013.11.036
51. F. Boorboor Ajdari, E. Kowsari, M. Niknam Shahrak, A. Ehsani, Z. Kiaei, H. Torkzaban, M. Ershadi, S. Kholghi Eshkalak, V. Haddadi-Asl, A. Chinnappan and S. Ramakrishna, *Coord. Chem. Rev.*, **422**, 213441 (2020); https://doi.org/10.1016/j.ccr.2020.213441
52. A.G. Pandolfo and A.F. Hollenkamp, *J. Power Sources*, **157**, 11 (2006); https://doi.org/10.1016/j.jpowsour.2006.02.065
53. D. Das, D.P. Samal and B.C. Meikap, *J. Chem. Eng. Process Technol.*, **6**, 100248 (2015); https://doi.org/10.4172/2157-7048.1000248
54. M.A.F. Mazlan, Y. Uemura, S. Yusup, F. Elhassan, A. Uddin, A. Hiwada and M. Demiya, *Procedia Eng.*, **148**, 530 (2016); https://doi.org/10.1016/j.proeng.2016.06.549
55. J. Wang and S. Kaskel, *J. Mater. Chem.*, **22**, 23710 (2012); https://doi.org/10.1039/c2jm34066f
56. T. Exner, M. Ahuja and L. Ellwood, *Clin. Chem. Lab. Med.*, **57**, 690 (2019); https://doi.org/10.1515/cclm-2018-0967
57. L.L. Zhang and X.S. Zhao, *Chem. Soc. Rev.*, **38**, 2520 (2009); https://doi.org/10.1039/b813846j
58. D. Weingarth, A. Foelske-Schmitz and R. Kotz, *J. Power Sources*, **225**, 84 (2013); https://doi.org/10.1016/j.jpowsour.2012.10.019
59. S.Y. Lim, W. Shen and Z. Gao, *Chem. Soc. Rev.*, **44**, 362 (2015); https://doi.org/10.1039/C4CS00269E
60. K. Kakaei, S. Khodadoost, M. Gholipour and N. Shouraei, *J. Phys. Chem. Solids*, **148**, 109753 (2021); https://doi.org/10.1016/j.jpcs.2020.109753
61. X. Jian, H.M. Yang, J.G. Li, E. Zhang, L. Cao and Z. Liang, *Electrochim. Acta*, **228**, 483 (2017); https://doi.org/10.1016/j.electacta.2017.01.082
62. Y. Zhu, Z. Wu, M. Jing, H. Hou, Y. Yang, Y. Zhang, X. Yang, W. Song, X. Jia and X. Ji, *J. Mater. Chem. A Mater. Energy Sustain.*, **3**, 866 (2015); https://doi.org/10.1039/C4TA05507A
63. L. Lv, Y. Fan, Q. Chen, Y. Zhao, Y. Hu, Z. Zhang, N. Chen and L. Qu, *Nanotechnology*, **25**, 235401 (2014); https://doi.org/10.1088/0957-4484/25/23/235401
64. S. Sahoo, A.K. Satpati, P.K. Sahoo and P.D. Naik, *ACS Omega*, **3**, 17936 (2018); https://doi.org/10.1021/acsomega.8b01238
65. Y. Zhou and Y. Xie, *J. Solid State Electrochem.*, **22**, 2515 (2018); https://doi.org/10.1007/s10008-018-3964-5
66. H. Lv, Y. Yuan, Q. Xu, H. Liu, Y.G. Wang and Y. Xia, *J. Power Sources*, **398**, 167 (2018); https://doi.org/10.1016/j.jpowsour.2018.07.059
67. J. Li, X. Yun, Z. Hu, L. Xi, N. Li, H. Tang, P. Lu and Y. Zhu, *J. Mater. Chem. A Mater. Energy Sustain.*, **7**, 26311 (2019); https://doi.org/10.1039/C9TA08151H
68. J.S. Wei, H. Ding, P. Zhang, Y.F. Song, J. Chen, Y.G. Wang and H.M. Xiong, *Nano Micro Small*, **12**, 5927 (2016); https://doi.org/10.1002/smll.201602164
69. Y. Wei, X. Zhang, X. Wu, D. Tang, K. Cai, Q. Zhang and Z. Qingguo, *RSC Adv.*, **6**, 39317 (2016); https://doi.org/10.1039/C6RA02730J
70. F. Markoulidis, C. Lei, C. Lekakou, E. Figgemeier, D. Duff, S. Khalil, B. Martorana and I. Cannavaro, *IOP Conf. Ser.: Mater. Sci. Eng.*, **40**, 012021 (2012); https://doi.org/10.1088/1757-899X/40/1/012021
71. J. Saleem, U.B. Shahid, M. Hijab, H. Mackey and G. McKay, *Biomass Convers. Biorefin.*, **9**, 775 (2019); https://doi.org/10.1007/s13399-019-00473-7
72. N. Job, R. Pirard, J. Marien and J.-P. Pirard, *Carbon*, **42**, 619 (2004); https://doi.org/10.1016/j.carbon.2003.12.072
73. A. Allahbakhsh and A.R. Bahramian, *Nanoscale*, **7**, 14139 (2015); https://doi.org/10.1039/C5NR03855C
74. A. Elkhatat and S.A. Al-Muhtaseb, *Adv. Mater.*, **23**, 2887 (2011); https://doi.org/10.1002/adma.201100283
75. W. Zhang, S.-H. Huang, C. Zhou, G. Cao, F. Kang and Y. Yang, *J. Mater. Chem.*, **22**, 7158 (2012); https://doi.org/10.1039/c2jm16276h
76. W.C. Chen, T.C. Wen and H. Teng, *Electrochim. Acta*, **48**, 641 (2003); https://doi.org/10.1016/S0013-4686(02)00734-X
77. L.F. Chen, X.D. Zhang, H.W. Liang, M. Kong, Q.F. Guan, P. Chen, Z.Y. Wu and S.H. Yu, *ACS Nano*, **6**, 7092 (2012); https://doi.org/10.1021/nn302147s
78. L. Qie, W. Chen, H. Xu, X. Xiong, Y. Jiang, F. Zou, X. Hu, Y. Xin, Z. Zhang and Y. Huang, *Energy Environ. Sci.*, **6**, 2497 (2013); https://doi.org/10.1039/c3ee41638k
79. X.Y. Chen, C. Chen, Z.J. Zhang, D.H. Xie, X. Deng and J.W. Liu, *J. Power Sources*, **230**, 50 (2013); https://doi.org/10.1016/j.jpowsour.2012.12.054

80. H. Guo and Q. Gao, *J. Power Sources*, **186**, 551 (2009); https://doi.org/10.1016/j.jpowsour.2008.10.024
81. Q. Wang, J. Yan, Y. Wang, T. Wei, M. Zhang, X. Jing and Z. Fan, *Carbon*, **67**, 119 (2014); https://doi.org/10.1016/j.carbon.2013.09.070
82. M. Liu, L. Gan, W. Xiong, Z. Xu, D. Zhu and L. Chen, *J. Mater. Chem.*, **2**, 2555 (2014); https://doi.org/10.1039/C3TA14445C
83. V. Augustyn, P. Simon and B. Dunn, *Energy Environ. Sci.*, **7**, 1597 (2014); https://doi.org/10.1039/c3ee44164d
84. E. Frackowiak, K. Jurewicz, S. Delpeux and F. Beguin, *J. Power Sources*, **97–98**, 822 (2001); https://doi.org/10.1016/S0378-7753(01)00736-4
85. K. Khan, A.K. Tareen, M. Aslam, A. Mahmood, Q. Khan, Y. Zhang, Z. Ouyang, Z. Guo and H. Zhang, *Prog. Solid State Chem.*, **58**, 100254 (2020); https://doi.org/10.1016/j.progsolidstchem.2019.100254
86. A.M. Saleem, V. Desmaris and P. Enoksson, *J. Nanomater.*, **2016**, Article id 1537269 (2016); https://doi.org/10.1155/2016/1537269
87. N.R. Chodankar, H.D. Pham, A.K. Nanjundan, J.F. Fernando, K. Jayaramulu, D. Golberg, Y.K. Han and D.P. Dubal, *Nano Micro. Small*, **16**, 2002806 (2020); https://doi.org/10.1002/smll.202002806
88. D. Majumdar, *Mater. Sci. Res. India*, **15**, 30 (2018); https://doi.org/10.13005/msri/150104
89. B.S. Singu, U. Male, S.E. Hong and K.R. Yoon, *Ionics*, **22**, 1485 (2016); https://doi.org/10.1007/s11581-016-1669-2
90. R.M. Obodo, N.M. Shinde, U.K. Chime, S. Ezugwu, A.C. Nwanya, I. Ahmad, M. Maaza, P. Ejikeme and F.I. Ezema, *Curr. Opin. Electrochem.*, **21**, 242 (2020); https://doi.org/10.1016/j.coelec.2020.02.022
91. Z. Zhao, T. Shen, Z. Liu, Q. Zhong and Y. Qin, *J. Alloys Compd.*, **812**, 152124 (2020); https://doi.org/10.1016/j.jallcom.2019.152124
92. T. Liu, L. Finn, M. Yu, H. Wang, T. Zhai, X. Lu, Y. Tong and Y. Li, *Nano Lett.*, **14**, 2522 (2014); https://doi.org/10.1021/nl500255v
93. M. Mastragostino, C. Arbizzani and F. Soavi, *Solid State Ion.*, **148**, 493 (2002); https://doi.org/10.1016/S0167-2738(02)00093-0
94. D.W. Wang, F. Li, J. Zhao, W. Ren, Z.G. Chen, J. Tan, Z.S. Wu, I. Gentle, G.Q. Lu and H.M. Cheng, *ASC Nano*, **3**, 1745 (2009); https://doi.org/10.1021/nn900297m
95. Z. Qiu, B.A. Hammer and K. Mullen, *Prog. Polym. Sci.*, **100**, 101179 (2020); https://doi.org/10.1016/j.progpolymsci.2019.101179
96. C. Li, H. Bai and G. Shi, *Chem. Soc. Rev.*, **38**, 2397 (2009); https://doi.org/10.1039/b816681c
97. I. Shown, A. Ganguly, L.C. Chen and K.H. Chen, *Energy Sci. Eng.*, **3**, 2 (2015); https://doi.org/10.1002/ese3.50
98. S.A. Ebrahim, M.E. Harb, M.M. Soliman and M.B. Tayel, *J. Taibah Univ. Sci.*, **10**, 281 (2016); https://doi.org/10.1016/j.jtusci.2015.07.004
99. S.R. Sivakkumar, W.J. Kim, J.A. Choi, D.R. MacFarlane, M. Forsyth and D.W. Kim, *J. Power Sources*, **171**, 1062 (2007); https://doi.org/10.1016/j.jpowsour.2007.05.103
100. H. Li, J. Wang, Q. Chu, Z. Wang, F. Zhang and S. Wang, *J. Power Sources*, **190**, 578 (2009); https://doi.org/10.1016/j.jpowsour.2009.01.052
101. Y.S. Lim, Y.P. Tan, H.N. Lim, N.M. Huang, W.T. Tan, M.A. Yarmo and C.Y. Yin, *Ceram. Int.*, **40**, 3855 (2014); https://doi.org/10.1016/j.ceramint.2013.08.026
102. G. Shi, M. Rouabhia, Z. Wang, L.H. Dao and Z. Zhang, *Biomaterials*, **25**, 2477 (2004); https://doi.org/10.1016/j.biomaterials.2003.09.032
103. A. Yagan, *Int. J. Electrochem. Sci.*, **14**, 3978 (2019); https://doi.org/10.20964/2019.04.12
104. X. Jiao, C. Zhang and Z. Yuan, *ACS Appl. Mater. Interfaces*, **10**, 41299 (2018); https://doi.org/10.1021/acsami.8b13503
105. M. Rajesh, C.J. Raj, B.C. Kim, B.B. Cho, J.M. Ko and K.H. Yu, *Electrochim. Acta*, **220**, 373 (2016); https://doi.org/10.1016/j.electacta.2016.10.118
106. M. Jaymand, M. Hatamzadeh and Y. Omidi, *Prog. Polym. Sci.*, **47**, 26 (2015); https://doi.org/10.1016/j.progpolymsci.2014.11.004
107. A. Laforgue, P. Simon, C. Sarrazin and J.F. Fauvarque, *J. Power Sources*, **80**, 142 (1999); https://doi.org/10.1016/S0378-7753(98)00258-4
108. H. Zhang, Z. Hu, M. Li, L. Hu and S. Jiao, *J. Mater. Chem. A Mater. Energy Sustain.*, **2**, 17024 (2014); https://doi.org/10.1039/C4TA03369H
109. K.L. Knoche, D.P. Hickey, R.D. Milton, C.L. Curchoe and S.D. Minteer, *ACS Energy Lett.*, **1**, 380 (2016); https://doi.org/10.1021/acsenergylett.6b00225
110. A. Burke, *Electrochim. Acta*, **53**, 1083 (2007); https://doi.org/10.1016/j.electacta.2007.01.011
111. K. Naoi and P. Simon, *Electrochem. Soc. Interface*, **17**, 34 (2008); https://doi.org/10.1149/2.F04081IF
112. T. Chen and L. Dai, *Mater. Today Commun.*, **16**, 272 (2013); https://doi.org/10.1016/j.mattod.2013.07.002
113. Z. Wang, M. Zhu, Z. Pei, Q. Xue, H. Li, Y. Huang and C. Zhi, *Mater. Sci. Eng. Rep.*, **139**, 100520 (2020); https://doi.org/10.1016/j.mser.2019.100520
114. J. Wang, Y. Xu, X. Sun, X. Li and X. Du, *J. Solid State Electrochem.*, **12**, 947 (2008); https://doi.org/10.1007/s10008-007-0439-5
115. P. Saikia, K. Dutta, A.K. Guha, S.K. Dolui, P. Barman and L.J. Borthakur, *Mater. Chem. Phys.*, **258**, 123786 (2021); https://doi.org/10.1016/j.matchemphys.2020.123786
116. S. Sundriyal, V. Shrivastav, S. Mishra and A. Deep, *Int. J. Hydrogen Energy*, **45**, 30859 (2020); https://doi.org/10.1016/j.ijhydene.2020.08.075
117. J. Chen, Y. Wang, J. Cao, L. Liao, Y. Liu, Y. Zhou, J.H. Ouyang, D. Jia, M. Wang, X. Li and Z. Li, *Electrochim. Acta*, **361**, 137036 (2020); https://doi.org/10.1016/j.electacta.2020.137036
118. X. Deng, X. Bai, Z. Cai, M. Huang, X. Chen, B. Huang and Y. Chen, *J. Mater. Res. Technol.*, **9**, 8544 (2020); https://doi.org/10.1016/j.jmrt.2020.05.130
119. H.M. Yadav, S. Ramesh, K.A. Kumar, S. Shinde, S. Sandhu, A. Sivasamy, N.K. Shrestha, H.S. Kim, H.S. Kim and C. Bathula, *Polym. Test.*, **89**, 106727 (2020); https://doi.org/10.1016/j.polymertesting.2020.106727
120. S. Arunachalam, B. Kirubasankar, D. Pan, H. Liu, C. Yan, Z. Guo and S. Angaiah, *Green Energy Environ.*, **5**, 259 (2020); https://doi.org/10.1016/j.gee.2020.07.021
121. B.E. Conway and W.G. Pell, *J. Solid State Electrochem.*, **7**, 637 (2003); https://doi.org/10.1007/s10008-003-0395-7
122. Y. Liu, D. He, H. Wu, J. Duan and Y. Zhang, *Electrochim. Acta*, **164**, 154 (2015); https://doi.org/10.1016/j.electacta.2015.01.223
123. P.C. Chen, G. Shen, Y. Shi, H. Chen and C. Zhou, *ACS Nano*, **4**, 4403 (2010); https://doi.org/10.1021/nn100856y
124. Y. Huang, T. Shi, S. Jiang, S. Cheng, X. Tao, Y. Zhong, G. Liao and Z. Tang, *Sci. Rep.*, **6**, 38620 (2016); https://doi.org/10.1038/srep38620
125. X. Zhou, Q. Chen, A. Wang, J. Xu, S. Wu and J. Shen, *ACS Appl. Mater. Interfaces*, **8**, 3776 (2016); https://doi.org/10.1021/acsami.5b10196
126. L. Su, L. Gong, X. Wang and H. Pan, *Int. J. Energy Res.*, **40**, 763 (2016); https://doi.org/10.1002/er.3480
127. S.G. Krishnan, M. Harilal, B. Pal, I.I. Misnon, C. Karuppiah, C.C. Yang and R. Jose, *J. Electroanal. Chem. (Lausanne)*, **805**, 126 (2017); https://doi.org/10.1016/j.jelechem.2017.10.029
128. S.A. Pawar, D.S. Patil and J.C. Shin, *Electrochim. Acta*, **259**, 664 (2018); https://doi.org/10.1016/j.electacta.2017.11.006
129. J. Sun, X. Du, R. Wu, Y. Zhang, C. Xu and H. Chen, *ACS Appl. Energy Mater.*, **3**, 8026 (2020); https://doi.org/10.1021/acsaem.0c01458
130. N. Li, Y. Du, Q.P. Feng, G.W. Huang, H.M. Xiao and S.Y. Fu, *ACS Appl. Mater. Interfaces*, **9**, 44828 (2017); https://doi.org/10.1021/acsami.7b14271
131. R. Sahoo, T.H. Lee, D.T. Pham, T.H. Luu and Y.H. Lee, *ACS Nano*, **13**, 10776 (2019); https://doi.org/10.1021/acsnano.9b05605